

A New Construction of Nonbinary Polar Codes with Two-stage Polarization

Peiyao Chen*, Baoming Bai*, and Xiao Ma†

*State Key Laboratory of Integrated Services Networks, Xidian University, Xi'an 710071, China

†School of Data and Computer Science, Sun Yat-sen University, Guangzhou 510006, China

Email: pychen@stu.xidian.edu.cn, bmbai@mail.xidian.edu.cn, maxiao@mail.sysu.edu.cn

Abstract—In this paper, we propose a new class of nonbinary polar codes with two-stage polarization, where the outer polarization (symbol-level polarization) kernel is a nonbinary matrix resembling Arikan's kernel, and the inner polarization (bit-level polarization) kernel is a properly designed binary matrix. The encoder/decoder of the proposed nonbinary polar codes have the same structure as the original binary polar codes, admitting an easily configurable and flexible implementation. This is an obvious advantage over the nonbinary polar codes based on Reed-Solomon (RS) codes. Simulation results show that, compared with modified RS-based polar codes, our proposed nonbinary polar codes can achieve similar performance but with a smaller list size. When compared with binary polar codes, the proposed nonbinary polar codes exhibit better performance and lower decoding latency (benefitted from the fact that multiple bits can be decoded as a symbol simultaneously).

I. INTRODUCTION

Binary polar codes, proposed by Arikan [1], were proved to be able to achieve the symmetric-capacity of binary-input discrete memoryless channels (DMCs) with explicit coding structures as well as low encoding and decoding complexity. Polarization effect exists by using nested transformations with the binary kernel $\mathbf{F}_2 = \begin{bmatrix} 1 & 0 \\ 1 & 1 \end{bmatrix}$ (called Arikan's kernel) in conjunction with a successive cancellation (SC)-based decoder. As the code length N tends to infinity, bit-channels polarize to be either nearly noiseless or useless, and the capacity can be approached by employing only the noiseless bit-channels for data transmission. It was shown that bit-channels can also be polarized with such a generator matrix that none of its column permutations is an upper triangle matrix [2]. Thus the original polar codes can be generalized by applying different kernels. The probability of block error for polar codes under SC decoding is found to be $\mathcal{O}(2^{-N^\beta})$ for any $\beta < \gamma$, where γ denotes the exponent of the kernel matrix [2]. The exponent γ of Arikan's kernel is 0.5, which can be improved by considering larger or nonbinary matrices [2]. Therefore, BCH-generator-matrices as polarization kernels were considered in [2], which yields an exponent greater than 0.5 at size 16×16 . Binary kernels with maximum exponents of dimensions up to sixteen were provided in [3].

Another way to increase the exponent is to extend binary polar codes to a nonbinary setting. In [4], Şaşıoğlu *et al.* proved that nonbinary polar codes with arbitrary finite input-alphabet sizes can achieve symmetric-capacity by decomposing underlying symbol channels into a set of subchannels

with prime input alphabet sizes, and they also showed that all DMCs can be polarized by randomized constructions. In 2014, Chiu [5] proposed a new approach, by using channel symbol permutations, to prove that polar codes polarize arbitrary q -ary input randomized channels. Nonbinary polar codes based on an $\ell \times \ell$ q -ary Reed-Solomon (RS) matrix $\mathbf{G}_{RS}(q, \ell)$ were proposed by Mori and Tanaka [6], which have exponents of order $\log(\ell!)/(\ell \log \ell)$ for all $\ell \leq q$ and can be made arbitrarily close to 1 as ℓ becomes large. In 2016, Cheng [7] *et al.* applied a four-dimensional RS matrix over the finite field $\text{GF}(4)$ as the kernel and showed that better error-correcting performance can be achieved compared with binary polar codes.

In this paper, we propose a new class of nonbinary polar codes with two-stage polarization. The outer polarization for symbol-level, referred to as *multiplicative repetition-based construction*, is based on a 2×2 q -ary matrix $\begin{bmatrix} 1 & 0 \\ \beta & 1 \end{bmatrix}$, where $\beta \neq 0$ acts as a multiplier and may vary for nested Kronecker operations. The inner polarization for bit-level, referred to as *polarization mapping*, is then applied to each coded symbol to further intensify the polarization. With this two-stage polarization, a q -ary input channel is treated as several binary input channels. As a result, *partially-frozen symbols* may arise. That is, there may exist symbols containing both frozen bits and active bits. This is different from existing constructions, in which a symbol is either *fully-frozen* or *fully-active*. An initial motivation of such a hybrid construction is to disperse information bits to more symbols, which may benefit from high order modulations. The partially-frozen symbol can be further utilized to improve the error-correcting performance by an *active-check construction*. An efficient successive cancellation list (SCL) decoding is also introduced for the proposed polar codes, which has a similar structure to that of the Arikan's polar codes [8], [9]. This is an obvious advantage over the existing RS-generator-matrix based polar codes, which require much more computations than ours due to their very different decoding structure from that of the original polar codes. In addition, with the proposed code structure, lower latency can be achieved compared with binary polar codes. Simulation results show that the proposed codes perform better than binary polar codes with BPSK. Simulation results also show that the performance gain can be increased with the increase of the field order. Moreover, the proposed codes also exhibit an outstanding performance with high-order modulations.

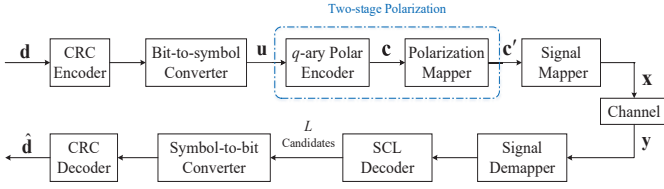


Fig. 1. System model for nonbinary polar codes.

II. SYSTEM MODEL

Let $\text{GF}(q)$ be the finite field with $q = 2^m$, where m is a positive integer greater than unity. Let α be a primitive element of $\text{GF}(q)$. Then $\alpha^{-\infty} = 0, \alpha, \alpha^2, \dots, \alpha^{q-2}$ form all the elements of $\text{GF}(q)$. Each element $\alpha^i \in \text{GF}(q)$ can be represented by an m -tuple over $\text{GF}(2)$.

The system model under consideration is depicted in Fig. 1. The q -ary polar encoder accepts as input a q -ary sequence \mathbf{u} of length n or, equivalently, a binary sequence of length $N = nm$. This input sequence \mathbf{u} is formed as follows. First, a binary sequence \mathbf{d} of length K is encoded by a CRC-encoder; the checked sequence is then formatted as a binary sequence of length N by inserting properly frozen bits and active-check bits according to the code construction; finally, the binary sequence is converted into the symbol sequence $\mathbf{u} = (u_1, u_2, \dots, u_n)$ with $u_i \in \text{GF}(q)$ ($1 \leq i \leq n$) as usual. To intensify the polarization, a polarization mapper is applied to each coded symbol $c_i \in \text{GF}(q)$ ($1 \leq i \leq n$) before the signal mapping. Apparently, the overall code rate $R = K/N$.

Suppose that a T -dimensional signal constellation \mathcal{S} of size $M = |\mathcal{S}|$ is used. A signal mapper maps the polar coded symbols c_i to modulated symbols $\mathbf{x}_i \in \mathcal{S}$, $1 \leq i \leq \frac{mn}{\log_2 M}$. Without loss of generality, we assume that mn is a multiple of $\log_2 M$. If necessary, zero bits are padded to the coded symbols. With the assumption that \mathbf{x}_i are transmitted over the AWGN channel, the received symbols \mathbf{y}_i are given by

$$\mathbf{y}_i = \mathbf{x}_i + \mathbf{n}_i, \quad 1 \leq i \leq \frac{mn}{\log_2 M} \quad (1)$$

where $\mathbf{n}_i = (n_{i,1}, n_{i,2}, \dots, n_{i,T})$ and $n_{i,j} \sim \mathcal{N}(0, N_0/2)$ are independent and identically distributed Gaussian random variables with zero mean and variance $N_0/2$ per dimension. At the receiver, the demapper computes posteriori probabilities (APPs) and delivers them to the SCL decoder. In the SCL decoder, L best paths are considered at each decoding stage. Finally, the L candidates from SCL decoder are checked by a CRC decoder successively, and the one with the best metric among the candidates which can pass the CRC detection is determined as the estimate $\hat{\mathbf{d}}$.

Denote the average transmitted energy per symbol by $E_s = \mathbb{E}[\|\mathbf{x}_i\|^2]$. Then the average received SNR is given by $\text{SNR} = \frac{E_s}{T \cdot N_0/2} = \frac{2}{T} \cdot \frac{E_b R \cdot \log_2 M}{N_0}$, where E_b denotes the average energy per information bit.

III. NONBINARY POLAR CODES WITH TWO-STAGE POLARIZATION

A. Symbol-Level Polarization with MR Construction

We extend binary polar codes to nonbinary polar codes by considering a 2×2 q -ary kernel given by

$$\mathbf{F}_q = \begin{bmatrix} 1 & 0 \\ \alpha^i & 1 \end{bmatrix},$$

where $\alpha^i \in \text{GF}(q) \setminus \{0\}$. With \mathbf{F}_q as the generator matrix, for each $\mathbf{u} = (u_1, u_2) \in [\text{GF}(q)]^2$, we have the coded sequence $\mathbf{c} = (c_1, c_2) = \mathbf{u}\mathbf{F}_q = (u_1 + \alpha^i u_2, u_2)$. In the case of $\alpha^i = 1$, \mathbf{F}_q has the same form as Arkan's, and u_2 is repeated once and then superimposed on u_1 . In the nonbinary case with $\alpha^i \neq 1$, we see $\alpha^i u_2$ is a multiplicative repetition of u_2 . For this reason, we call the construction *multiplicative repetition* (MR)-based construction for convenience.

Let $\mathbf{G}_2 = \mathbf{F}_q$ and α^{i_r} represent the multiplier for the r -th Kronecker operation. Then the generator matrix with the code length $n = 2^r$ is given by

$$\mathbf{G}_n = \mathbf{B}_n \mathbf{F}_q^{\otimes r} = \mathbf{B}_n \begin{bmatrix} \mathbf{F}_q^{\otimes(r-1)} & 0 \\ \alpha^{i_r} \mathbf{F}_q^{\otimes(r-1)} & \mathbf{F}_q^{\otimes(r-1)} \end{bmatrix}, r \geq 2,$$

where \mathbf{B}_n is a permutation matrix for bit-reversal operation, and the multiplier α^{i_j} ($1 \leq j \leq r$) is randomly chosen from the nonzero elements set \mathcal{X}^* of $\text{GF}(q)$. All multipliers are known both to the transmitter and to the receiver.

The MR-based construction is similar to the permutation construction proposed in [4]. Thus, with the Proposition 1 in [4], we can prove (omitted here due to space limitation) that the MR-based transformation polarize q -ary discrete memoryless channels. This is referred to as *symbol-level polarization*.

B. Bit-Level Polarization with Polarization Mapping

Different from conventional nonbinary polar codes, in which only symbol-level polarization is discussed and the construction is based on the symbol-level, we introduce the bit-level polarization by a polarization mapping to each coded symbol.

The mapping pattern is based on an $m \times m$ binary polarization matrix \mathbf{M}_m with the maximum polarization rate among the matrices of the same size. Decompose each q -ary input channel into m bit-channels by treating each coded symbol $c_i \in \text{GF}(q)$ as a binary vector $\mathbf{c}_i = (c_i[1], \dots, c_i[m])$. With the matrix \mathbf{M}_m , each coded symbol c_i is mapped to $\mathbf{c}'_i = \mathbf{c}_i \cdot \mathbf{M}_m$. For example, assuming that $q = 4$ and $\mathbf{M}_2 = \begin{bmatrix} 1 & 0 \\ 1 & 1 \end{bmatrix}$, we have $\mathbf{c}'_i = (c'_i[1], c'_i[2]) = (c_i[1] + c_i[2], c_i[2])$. With this process, bits in the same symbol become dependent. Similar to binary polar codes, it can be proved that polarization exists in the decomposed bit-channels by regarding the mapping process as a binary encoding with the polarization matrix. It is worth noting that, without the polarization mapping, the choice of information index set via bit-channel reliabilities will be equivalent to that via symbol-channel reliabilities.

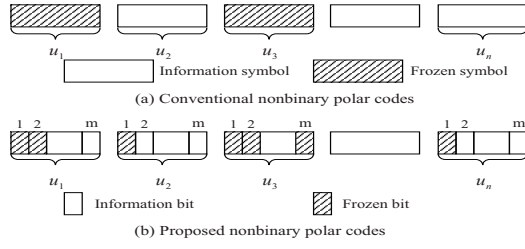


Fig. 2. Input formats of the bits/symbols to the encoder.

C. Code Construction

Our code construction is different from the conventional q -ary code construction in the sense that we sort bit-channel reliabilities. This effective construction is attributed to the existence of the polarization mapping. Assume that $p(y|u)$, $u \in \text{GF}(q)$, represents the channel conditional probabilities given by the demapper. Due to the similar structure to binary polar codes, the recursive formulas for the SC decoding are given as

$$\begin{aligned}
 & p_{\lambda}^{(2i-1)}(y_1^{\Lambda}, u_1^{2i-2} | u_{2i-1}) \\
 &= \sum_{u_{2i}} \frac{1}{q} \{ p_{\lambda-1}^{(i)}(y_1^{\Lambda/2}, u_{1, \text{odd}}^{2i-2} \oplus \alpha^{i+1} u_{1, \text{even}}^{2i-2} | u_{2i-1} \oplus \alpha^{i_t} u_{2i}) \\
 & \quad \cdot p_{\lambda-1}^{(i)}(y_{\Lambda/2+1}^{\Lambda}, u_{1, \text{even}}^{2i-2} | u_{2i}) \}, \\
 & p_{\lambda}^{(2i)}(y_1^{\Lambda}, u_1^{2i-1} | u_{2i}) \\
 &= \frac{1}{q} p_{\lambda-1}^{(i)}(y_1^{\Lambda/2}, u_{1, \text{odd}}^{2i-2} \oplus \alpha^{i+1} u_{1, \text{even}}^{2i-2} | u_{2i-1} \oplus \alpha^{i_t} u_{2i}) \\
 & \quad \cdot p_{\lambda-1}^{(i)}(y_{\Lambda/2+1}^{\Lambda}, u_{1, \text{even}}^{2i-2} | u_{2i}), \quad (2)
 \end{aligned}$$

where $1 \leq \lambda \leq \log_2 n$, $1 \leq 2i-1 \leq \lambda$, $\Lambda = 2^\lambda$, $t = \log_2 n - \lambda + 1$ and $p_0^{(1)}(y|u) = p(y|u)$.

A genie-aided SC decoder is used to compute the bit-channel reliabilities for q -ary polar codes with \mathbf{G}_n , where mn information bits are uniformly generated. For $1 \leq i \leq n$ and $1 \leq j \leq m$, denote $I_{i,j} = m(i-1) + j$. The j -th bit-channel within the i -th symbol-channel is then referred to as the $I_{i,j}$ -th bit-channel, whose reliability is computed under the assumption that symbols u_1^{i-1} ($1 \leq i \leq n$) are available at the SC decoder. Denote the index set of bit-channels with the largest capacities by $\mathcal{F} \subseteq \{1, 2, \dots, mn\}$, whose size $|\mathcal{F}|$ is determined by the code rate. The bit-channels indexed by \mathcal{F} will be used to transmit active bits. Given this, frozen bits will be typically distributed as shown in Fig. 2(b).

We distinguish the symbols into three types, i.e., information symbols, partially-frozen symbols, and frozen symbols in terms of the number of active bits in a symbol. Both information symbols and partially-frozen symbols are known as unfrozen symbols, collectively denoted by \mathcal{A} . Then $\mathcal{A}^c = \{1, 2, \dots, n\} \setminus \mathcal{A}$ denote the set of frozen symbol indices, where for any $i \in \mathcal{A}^c$, all corresponding $I_{i,j} \notin \mathcal{F}$, $1 \leq j \leq m$.

The frozen bits in partially-frozen symbols can be used as active-check bits, facilitating the SCL decoder to detect and prune error paths in time. For this end, consider the symbols

with only one active bit, referred to as *one-bit* symbols, collectively denoted by $\mathcal{A}^* \subseteq \mathcal{A}$. Denote by $I_{i,\ell}$ and $I_{i,h}$ ($1 \leq \ell, h \leq m$) the bit-channel indices with lowest reliability and highest reliability for the i -th symbol, respectively. Let $i \in \mathcal{A}^*$, followed by $i' \in \mathcal{A}^*$, the next adjacent one-bit symbol (if any). We retransmit the $I_{i,h}$ -th bit (active bit in the i -th symbol) once as an active-check bit at the $I_{i',\ell}$ -th bit-channel. Then, at the decoder, the i' -th symbol is split by considering the constraint that the $I_{i',\ell}$ -th bit is equal to the $I_{i,h}$ -th decoded (estimated) bit. We call such a construction *active-check construction*.

D. Decoding Algorithm

We consider CRC-aided SCL decoding for the proposed q -ary polar codes. Assume that the maximum L decoding paths are kept at each decoding stage. Since a partially-frozen symbol can only take values from a subset of $\text{GF}(q)$, the decoding path for an unfrozen symbol is split into at most q branches. Then we choose the L most likely paths from all the possible extended paths ($\leq qL$) according to their path metrics. After SCL decoding, the decoder outputs the estimated information sequence given by the decoding path with the maximum path metric among the paths which can pass the CRC. The main CRC-aided SCL decoding algorithm for two-stage polarization-based polar codes is shown in Algorithm 1.

E. Decoding Latency

Let us first consider the latency of SC decoding. Denote by functions \mathbf{f} and \mathbf{g} the node update equations (2) and (3), respectively. According to [10], for binary polar codes with $N = 2^{\log_2 m} n$, $2N - 2$ clock cycles (CLKs) are required for the SC decoder, where both functions \mathbf{f} and \mathbf{g} can be carried out in a single CLK. For the proposed q -ary polar codes, $(n-1) \log_2 q$ CLKs are needed for the function \mathbf{f} due to $\log_2 q$ additions for each unit \mathbf{f} , and the number of CLKs required for the function \mathbf{g} is the same as that of binary cases. Thus, a total of $(n-1) \log_2 q + (n-1) = (m+1)(n-1)$ CLKs are required for the proposed q -ary SC decoder.

An L -size SCL decoder can be viewed as the combination of L copies of SC component decoders. In addition, the SCL decoder needs to sort qL (for worst case) path metrics and selects the L largest metrics for each decoded bit, thus, extra CLKs are required to carry out sorting and selecting functions. Using Bitonic sorter [11], the total number of stages is $S = \frac{1}{2} \log_2(qL)(\log_2(qL) + 1)$, where each stage contains $\frac{qL}{2}$ compare-and-select (CAS) units consisting of one comparator and a 2-to-2 MUX. Generally, an intermediate variable (or register) is required to swap two numbers resulting in 3 CLKs [12]. Since only unfrozen symbols require sorting and selecting functions, at most $3|\mathcal{A}|S = \frac{3}{2}|\mathcal{A}|(\log_2 L + m)(\log_2 L + m + 1)$ CLKs are needed for q -ary polar decoder to sort and select paths. For binary decoder, the number of unfrozen bits is $|\mathcal{F}|$. The CLKs required by SC-decoder and SCL-decoder for binary and q -ary polar codes are tabulated in Table I for comparison.

Algorithm 1: CRC – aided SCL Nonbinary Decoder

Input: received channel probabilities
Output: estimated source sequence

```

1  $r(\cdot) \leftarrow 0, a[\cdot] \leftarrow 0.$ 
2 for  $i = 1$  to  $n$  do
3   for  $l = 1$  to  $L$  do
4     if  $i \in \mathcal{A}^c$  then
5       Set  $\hat{u}_i(l) = 0$  and remain all paths.
6     else
7       if  $i \in \mathcal{A}^*$  then
8          $a[\ell] \leftarrow r(l), a[h] \leftarrow -1.$ 
9          $a[j] \leftarrow 0$ , for all  $j \in \{1, 2, \dots, m\} \setminus \{\ell, h\}.$ 
10        else
11           $a[j'] \leftarrow 0$ , for all
12             $j' \in \{j | I_{i,j} \in \{1, 2, \dots, mn\} \setminus \mathcal{F}\}.$ 
13           $a[j'] \leftarrow -1$ , for all  $j' \in \{j | I_{i,j} \in \mathcal{F}\}.$ 
14          • Compute the set  $\hat{\mathcal{A}}(l)$ :  $\hat{\mathcal{A}}(l) \leftarrow \phi.$ 
15          if  $a[j] < 0$ , for all  $1 \leq j \leq m$  then
16             $\hat{\mathcal{A}}(l) \leftarrow \{0, 1, \dots, q-1\}$ 
17          else
18            For all  $\beta \in \text{GF}(q)$  with vector form
19               $(\beta[1], \dots, \beta[m]).$ 
20            if  $\beta[j'] == a[j']$ , for all
21               $j' \in \{j | a[j] \geq 0, 1 \leq j \leq m\}$  then
22               $\hat{\mathcal{A}}(l) \leftarrow \hat{\mathcal{A}}(l) \cup \{\beta\}.$ 
23          • Calculate the conditional probabilities according to the
24            set  $\hat{\mathcal{A}}(l)$  using Eq.(2) and Eq.(3).
25   if  $i \in \mathcal{A}$  then
26     • Sort the conditional probabilities in descending order, and
27       select the  $L$  most likely paths with the largest probabilities.
28   if  $i \in \mathcal{A}^*$  then
29     for  $l = 1$  to  $L$  do
30        $r(l) \leftarrow \hat{u}_i[h](l).$ 
31 Find the most likely path which passes the CRC.

```

TABLE I
CLOCK CYCLES COMPARISON

Polar codes	SC-decoder	SCL-decoder
q -ary	$(m+1)(n-1)$	$(m+1)(n-1) + \frac{3}{2} \mathcal{A} (\log_2 L + m)(\log_2 L + m + 1)$
binary	$2^{\log_2 m+1}n - 2$	$2^{\log_2 m+1}n - 2 + \frac{3}{2} \mathcal{F} (\log_2 L + 1)(\log_2 L + 2)$

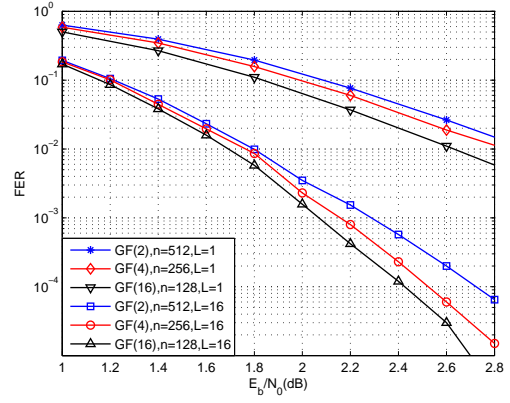
IV. NUMERICAL RESULTS AND ANALYSIS

In this section, error-correcting performances are provided for the proposed nonbinary (NB) polar codes, where both BPSK and high-order modulations over AWGN channels are considered. The polarization matrices

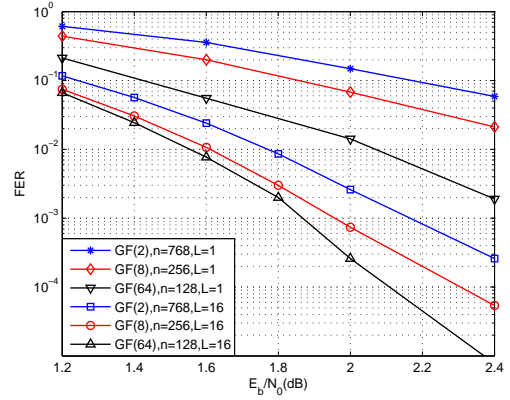
$$\mathbf{M}_2 = \begin{bmatrix} 1 & 0 \\ 0 & 1 \end{bmatrix}, \mathbf{M}_3 = \begin{bmatrix} 1 & 0 & 0 \\ 0 & 1 & 0 \\ 0 & 0 & 1 \end{bmatrix}, \mathbf{M}_4 = \begin{bmatrix} 1 & 0 & 0 & 0 \\ 0 & 1 & 0 & 0 \\ 0 & 0 & 1 & 0 \\ 0 & 0 & 0 & 1 \end{bmatrix}, \mathbf{M}_6 = \begin{bmatrix} 1 & 0 & 0 & 0 & 0 & 0 \\ 0 & 1 & 0 & 0 & 0 & 0 \\ 0 & 0 & 1 & 0 & 0 & 0 \\ 0 & 0 & 0 & 1 & 0 & 0 \\ 0 & 0 & 0 & 0 & 1 & 0 \\ 0 & 0 & 0 & 0 & 0 & 1 \end{bmatrix}$$

are applied for the polarization mapping of GF(4), GF(8), GF(16) and GF(64), respectively.

Example 1: Consider the proposed q -ary polar codes with BPSK over the AWGN channel. Two rate-1/2 codes with equivalent code length of $N=512$ and $N=768$ are simulated.



(a) $N = 512$



(b) $N = 768$

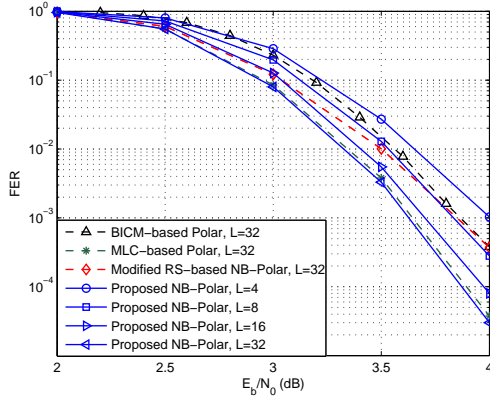
Fig. 3. Performance comparison between binary polar codes and nonbinary polar codes with BPSK over the AWGN channel: $|\mathcal{F}|$ is $N/2 + 8$, and $|\mathcal{A}|$ is 133 for GF(4), 66 for GF(16), 131 for GF(8), and 66 for GF(64).

In Fig. 3(a), both 4-ary polar codes and 16-ary polar codes are constructed by Monte-Carlo method at 1.7 dB. In Fig. 3(b), both 8-ary polar codes and 64-ary polar codes are constructed by Monte-Carlo method at 1.8 dB. The FER performance are given under both SC decoding and 8-bit CRC-aided SCL decoding method.

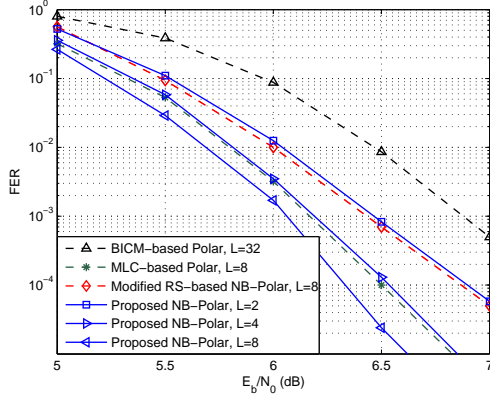
For reference, the performance of comparable binary polar codes, constructed by GA method at -1.59 dB, are also given in Fig. 3. The quasi-uniform puncturing (QUP) method in [13] is used to adapt the code length.

From Fig. 3, we can see that our proposed nonbinary polar codes outperform binary polar codes with BPSK over the AWGN channel. The coding gain is increased with the increase of the field order. Moreover, from Table I, it can be checked that the latency of our proposed nonbinary polar codes is lower than that of binary cases, and that can be decreased with the increase of the field order.

Example 2: Consider the proposed q -ary polar codes with 2^m -ary modulations over the AWGN channel. Rate-1/2 codes with two modulation schemes 16-QAM and 64-QAM are simulated. In Fig. 4(a), the proposed 16-ary polar codes with $N = 2048$ are constructed by Monte-Carlo method at 4.0 dB.



(a) 16-QAM



(b) 64-QAM

Fig. 4. Performance comparison with 16-QAM and 64-QAM over the AWGN channel.

In Fig. 4(b), the proposed 64-ary polar codes with $N = 1536$ are constructed by Monte-Carlo method at 5.0 dB. The 16-bit CRC-aided SCL decoding with various list sizes are applied.

For comparison, the performance of comparable modified RS-based q -ary polar codes $G_{RS}(q, 2)$ in [6] are also given in Fig. 4, where the codes are constructed by Monte-Carlo method at the aforementioned design-SNRs. Also considered for comparison are bit-interleaved coded-modulation (BICM) scheme [14][15] and multilevel coding (MLC) scheme [16][17] using comparable binary polar codes with 2^m -ary QAM, where the codes are constructed by Monte-Carlo method at 4.5 dB for 16-QAM and 6.0 dB for 64-QAM. For the BICM-based scheme, the bit-interleaver designed in [15] is applied, and the QUP method is used to adapt the code length. For the MLC-based scheme, m individual coding levels are employed. The rate allocations are obtained via the capacity rule in [16]. The SP labeling is applied to the MLC-based scheme, and Gray labeling is employed to other schemes.

From Fig. 4, we see that our proposed nonbinary polar codes combined with high-order modulations exhibit better performance than BICM-based scheme and can achieve sim-

ilar performance but with a smaller list size compared with modified RS-based polar codes. Under 64-QAM, compared with MLC-based scheme, about 0.2 dB gain can be obtained by our proposed polar codes with $L = 8$ at $\text{FER} = 10^{-4}$.

V. CONCLUSION

We have presented a new class of nonbinary polar codes constructed with two-stage polarization, where the symbol-level polarization is based on a q -ary kernel, which is a variation of Arkan's kernel, and the bit-level polarization is considered by using a polarization mapping with a designed binary matrix. Simulation results show that the proposed nonbinary polar codes perform better than binary polar codes with BPSK and high-order modulations over the AWGN channel. Furthermore, compared with modified RS-based polar codes, the proposed polar codes can achieve similar performance but with a smaller list size for high-order modulations.

REFERENCES

- [1] E. Arkan, "Channel polarization: A method for constructing capacity achieving codes for symmetric binary-input memoryless channels," *IEEE Trans. Inf. Theory*, vol. 55, no. 7, pp. 3051-3073, Jul. 2009.
- [2] S. Korada, E. Şaşıoğlu and R. Urbanke, "Polar Codes: Characterization of exponent, bounds, and constructions," *IEEE Trans. Inf. Theory*, vol. 56, no. 12, pp. 6253-6264, Dec. 2010.
- [3] H. P. Lin, S. Lin, and K. A. S. Abdel-Ghaffar, "Linear and nonlinear binary kernels of polar codes of small dimensions with maximum exponents," *IEEE Trans. Inf. Theory*, vol. 61, no. 10, pp. 5253-5270, Aug. 2015.
- [4] E. Şaşıoğlu, E. Telatar, and E. Arkan, "Polarization for arbitrary discrete memoryless channels," in *Proc. IEEE Inf. Theory Workshop*, pp. 144-148, Oct. 2009.
- [5] M. Chiu, "Non-binary polar codes with channel symbol permutations," in *Proc. IEEE Int. Symp. Inf. Theory & Its Applications*, pp. 433-437, Oct. 2014.
- [6] R. Mori, and T. Tanaka, "Non-binary polar codes using Reed-Solomon codes and algebraic geometry codes," in *Proc. IEEE Inf. Theory Workshop*, pp. 1-5, Sep. 2010.
- [7] N. Cheng, R. Zhang, and Y. Ge *et al.*, "Encoder and list decoder of Reed-Solomon kernel based polar codes," in *Proc. IEEE Int. Conf. Wireless Commun. & Signal Process.*, pp. 1-6, Oct. 2016.
- [8] I. Tal and A. Vardy, "List decoding of polar codes," in *Proc. IEEE Int. Symp. Inf. Theory*, pp. 1-5, Aug. 2011.
- [9] K. Chen, K. Niu, and J. R. Lin, "List successive cancellation decoding of polar codes," *Electronics Lett.*, vol. 48, no. 9, pp. 500-501, Apr. 2012.
- [10] C. Leroux, I. Tal, A. Vardy, and W. J. Gross, "Hardware architecture for successive cancellation decoding of polar codes," in *Proc. IEEE Int. Conf. Acoustics, Speech, and Signal Process.*, pp. 1665-1668, May. 2011.
- [11] A. Balatsoukas-Stimming, M. Parizi, and A. Burg, "On metric sorting for successive cancellation list decoding of polar codes," in *Proc. IEEE Int. Symp. Circuits and Systems*, pp. 1993-1996, Jun. 2015.
- [12] S. Shi, B. Han, J. Gao, and Y. Wang, "Enhanced successive cancellation list decoding of polar codes," *IEEE Commun. Lett.*, vol. 21, no. 6, pp. 1233-1236, Nov. 2017.
- [13] K. Niu, K. Chen, and J. R. Lin, "Beyond turbo codes: Rate-compatible punctured polar codes," in *Proc. IEEE Int. Conf. Commun.*, pp. 3423-3427, Jun. 2013.
- [14] K. Chen, K. Niu and J. Lin, "An efficient design of bit-interleaved polar coded modulation," in *Proc. IEEE Int. Symp. Personal Indoor and Mobile Radio Commun.*, Sep. 2013.
- [15] P. Chen, M. Xu, B. Bai, and X. Ma, "Design of polar coded 64-QAM," in *Proc. IEEE Int. Symp. Turbo Codes & Iterative Inf. Process.*, pp. 251-255, Sep. 2016.
- [16] M. Seidl, A. Schenk, C. Stierstorfer, and J. Huber, "Polar-coded modulation," *IEEE Trans. Commun.*, vol. 61, no. 10, pp. 4108-4119, Oct. 2013.
- [17] G. Böcherer, T. Prinz, P. Yuan, and F. Steiner, "Efficient polar code construction for higher-order modulation," in *Proc. IEEE Wireless Commun. and Networking Conference Workshops*, Mar. 2017.